

Progress in Predicting Ionic Cocrystal Formation: The Case of Ammonium Nitrate

Andrew J. Bennett^[a] and Adam J. Matzger^{*[a, b]}

Abstract: In contrast to the mature predictive frameworks applied to neutral cocrystals, ionic cocrystals, those including an ion pair, are difficult to design. Furthermore, they are generally excluded categorically from studies which correlate specific molecular properties to cocrystal formation, leaving the prospective ionic cocrystal engineer with few clear avenues to success. Herein ammonium nitrate, an energetic oxidizing salt, is targeted for cocrystallization in a potential coformer group selected based on likely interactions with the

nitrate ion as revealed in the Cambridge Structural Database; six novel ionic cocrystals were discovered. Molecular descriptors previously identified as being related to neutral cocrystal formation were examined across the screening group but showed no relationship with ionic cocrystal formation. High packing coefficient is shown to be a constant among the successful coformers in the set and is utilized to directly target two more successful coformers, bypassing the need for a large screening group.

Introduction

Knowledge-based approaches to identifying intermolecular interactions have been an essential tool in the production and study of cocrystals since the work of Desiraju on supramolecular synthons nearly 30 years ago.^[1–3] Despite major advances in computational prediction of cocrystal structure from first principles,^[4,5] knowledge-based approaches are firmly entrenched in the future of cocrystal design as new database analysis tools and machine learning algorithms are developed to analyze vast amounts of data and inform design choices.^[6–10] At the simplest level, a database approach to cocrystal design involves searching the Cambridge Structural Database^[11] (CSD) for the target molecule, recording the interactions it participates in, and then selecting a series of coformers for screening based on the observed synthon proclivities. A more involved approach may analyze the likelihood of specific synthons materializing in a given chemical environment based on synthon competition.^[12,13] Beyond functionality, various trends in molecular properties have been identified to aid in the selection of successful coformers and reduce the burden of

large-scale screening experiments; molecules with similar shape and polarity have been shown to be more likely to form cocrystals,^[14] while electrostatic potential maps have been used to match coformers based on hydrogen bond donor and acceptor strength.^[15–17]


In general, cocrystals have been studied extensively,^[18,19] but ionic cocrystals (other nomenclatures have been proposed),^[20] structures in which an ion pair has cocrystallized with a neutral non-liquid coformer, remain relatively rare.^[21] Ionic cocrystals have utility in pharmaceuticals^[22,23] and, more recently, energetic materials,^[24,25] but suffer from a paucity of experimental data. This limits the potential utility of database approaches to ionic cocrystal design. Further difficulty is encountered when attempting to assess coformers based on chemical properties; ionic cocrystals are often excluded categorically from studies on the trends that lead to cocrystallization, and no large-scale studies have yet been conducted to assess trends related to ionic cocrystal formation specifically. The aim of this work is twofold: to demonstrate a workaround strategy for enabling a database approach to cocrystal design for salts with limited data available, and to experimentally assess trends in ionic cocrystal formation with a target salt.


Results and Discussion

To assess trends in ionic cocrystallization, a target salt was screened for cocrystals with a set of 20 molecular coformers (Table 1). Ammonium nitrate (AN), an energetic oxidizer,^[26,27] was selected as the target salt. AN has applications in energetic formulations but is plagued by a near-room temperature phase transition and an accompanying change in volume, which complicates processing and storage.^[28] To select likely coformers for AN, the Cambridge Structural Database (CSD) was searched to evaluate the interactions that lead to AN cocrystallization. With only five AN ionic cocrystals in the CSD,^[29–31] three

[a] A. J. Bennett, Prof. Dr. A. J. Matzger
Department of Chemistry
University of Michigan
930 North University Ave, 48109 Ann Arbor, MI (USA)
E-mail: matzger@umich.edu

[b] Prof. Dr. A. J. Matzger
Macromolecular Science and Engineering Program
University of Michigan
48109 Ann Arbor, MI (USA)

 Supporting information for this article is available on the WWW under <https://doi.org/10.1002/chem.202300076>

 © 2023 The Authors. Chemistry - A European Journal published by Wiley-VCH GmbH. This is an open access article under the terms of the Creative Commons Attribution Non-Commercial License, which permits use, distribution and reproduction in any medium, provided the original work is properly cited and is not used for commercial purposes.

| Table 1. 20 molecular coformers screened for cocrystals with ammonium nitrate. | | |
|--|------------------------|--------------|
| ID | compound name | outcome |
| a | 2-pyridone | cocrystal |
| b | 4-cyanoimidazole | cocrystal |
| c | 4-pyridone | cocrystal |
| d | 5-amino-1,2,4-triazole | cocrystal |
| e | cyanuric acid | cocrystal |
| f | picolinic acid | cocrystal |
| g | 1h-1,2,4-triazole | no cocrystal |
| h | 2-nitroimidazole | no cocrystal |
| i | 3,5-diaminotriazole | no cocrystal |
| j | 3,5-dimethylpyrazole | no cocrystal |
| k | 4-chloropyrazole | no cocrystal |
| l | 5-aminotetrazole | no cocrystal |
| m | 5-nitro-1,2,4-triazole | no cocrystal |
| n | barbituric acid | no cocrystal |
| o | benzimidazole | no cocrystal |
| p | methyl benzimidazole | no cocrystal |
| q | parabanic acid | no cocrystal |
| r | pyrazole | no cocrystal |
| s | 2-methylimidazole | salt |
| t | imidazole | salt |

of which are inclusion compounds, the data are insufficient for design. Recently, a database approach targeting only ammonium interactions was successfully employed to produce a novel ammonium dinitramide:urea cocrystal,^[32] demonstrating the viability of designing ionic cocrystals based on interactions with only a single ion. To generate a sufficiently large dataset, a single ion approach to database searching was employed in the present work. Each ion was examined in structures with all counterions and their interactions documented individually to generate a list of structures in which the chosen ion participates in a cocrystal. This approach provides a significant increase to the data set size albeit with the disadvantage that persistent interactions between ammonium and nitrate cannot be accounted for. Previous work has examined the ammonium ion^[21,32] and therefore here the search focuses on the nitrate ion. The increase in data is significant; the CSD contains 123 ionic cocrystals involving a nitrate ion, including solvates of ionic cocrystals and excluding duplicate entries (Figure 1). About one third of these structures feature interactions (defined in CSD search parameters as Van der Waals radius overlap) between nitrate and an N–H functionality, making this the most prevalent interaction in the data set. Most of the remaining structures are inclusion compounds with cucurbiturils and crown ethers, the formation of which has previously been shown to rely on different parameters than traditional cocrystallization.^[14,33]

A set of 20 nitrogen heterocycles including cyclic amides and azoles were selected as potential coformers due to the presence of the target N–H functionality (Figure 2). Screening was carried out with a uniform method designed to provide each coformer with sufficient opportunity to form a cocrystal without any special considerations or experimental deviations. Several crystallization methods were employed for each coformer: cooling crystallization in water and in methanol, evaporative crystallization in methanol, slurry crystallization in acetonitrile, and liquid-assisted grinding with acetonitrile. Of

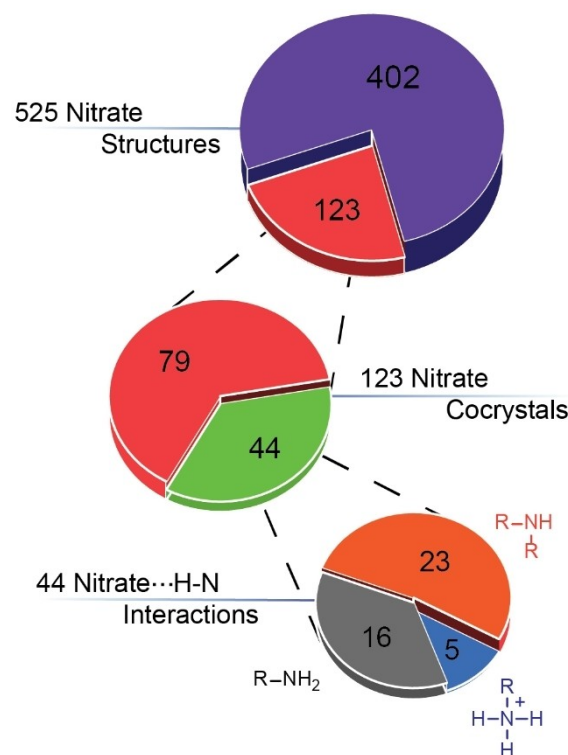


Figure 1. Classification of nitrate-containing structures within the CSD. In 44 out of 123 nitrate-containing cocrystals, nitrate interacts with an N–H functionality (See Supporting Information for search parameters).

the 20 chosen coformers, 2 showed acid-base reactivity with AN and yielded nitrate salts. Of the remaining 18, one third formed cocrystals with AN while the remainder returned the starting materials. This is a solid success for demonstrating the ability of the single ion approach to inform cocrystal design for salts with limited representation in the CSD. These are also the first instances of a nitrate hydrogen bonding with a neutral azolic N–H, a welcome addition to the scarcely populated toolbox of the ionic cocrystal engineer.

Although the single ion database approach was effective for providing an expanded dataset, an approach based purely on coformer functionality is incapable of explaining discrepancies in the preference of AN for certain coformers within the screening group. For example, 5-amino-1,2,4-triazole forms a cocrystal yet 5-aminotetrazole does not. Even taking into account the data previously gathered for the ammonium ion^[32] does little to explain these preferences as nitrogen heterocycles in general were found to interact favorably with ammonium. Amine-carbonyl functionalities including amides and ureas were previously identified as particularly favorable interaction sites for ammonium, and coformers containing these functionalities did form ionic cocrystals at a higher rate than the overall coformer group, suggesting some synergy between the separate database approaches for each ion. However, the failure of certain urea-containing coformers to form ionic cocrystals while very similar coformers succeeded (e.g., barbituric acid vs. cyanuric acid) still demands explanation. Thus, properties

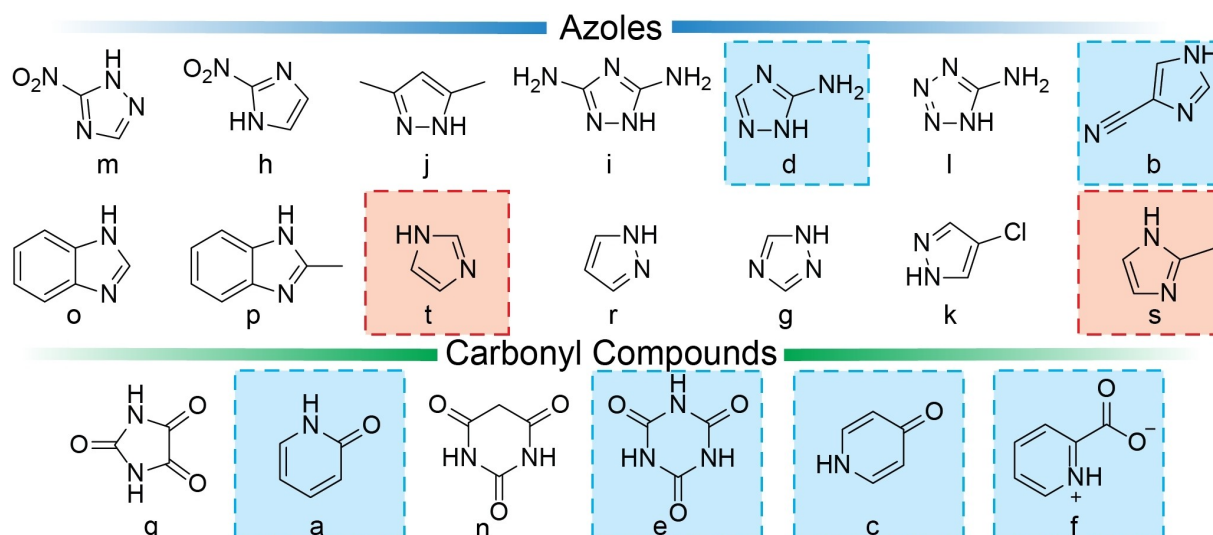


Figure 2. Screening group sorted by functionality type. Successful cocrystal formers are highlighted in blue and cofomers displaying acid-base reactivity are highlighted in red. Many of the cofomers that failed to generate cocrystals are structurally similar to successful ones, indicating that functionality alone is insufficient for explaining the preference of AN for certain cofomers.

previously identified as related to neutral molecular cocrystallization were applied to the cofomer preferences observed for AN. Molecular shape and polarity have been shown to have a strong correlation with cocrystal formation; a target molecule and cofomer with similar shape and polarity are more likely to form cocrystals than those with disparate values. Due to the potential for multiple ion pairing arrangements, the shape and polarity of a salt are ambiguous and thus cannot be compared directly to the cofomer. Narrowing the focus to compare the cofomer to a single ion is possible in cases with larger and more complex ions,^[34] but simple symmetric ions like ammonium and nitrate are essentially non-polar when considered individually, which is not a useful assessment of their actual electron distribution as a pair. However, because there is only one target salt (AN) in this study, examining the molecular properties of the cofomers alone is enough to assess any trends in successful cocrystallization.

Shape was assessed with two descriptors: ovality, and the ratio of the shortest side length to the longest side length (S/L). Polarity was assessed in terms of dipole moment, polar surface area (PSA), and FNO, a simplification of fractional polar volume obtained by dividing the combined number of oxygen and nitrogen atoms by the total number of heavy atoms in a molecule. Within the screening group, there is no obvious correlation between molecular shape or polarity and ability to form cocrystals with AN (Figure 3). Electrostatic potential has also been related to hydrogen bond donor/acceptor strength and likelihood of cocrystal formation. Electrostatic potential maps were generated for each cofomer in the screening group, and each was assessed in terms of maximum ($V_{s,max}$) and minimum ($V_{s,min}$) electrostatic potential, representing the strongest hydrogen bond donor and acceptor groups respectively. The difference (ΔV_s) in electrostatic potential across each molecule was also considered. No trend appears in any of these

metrics with regards to cocrystal formation. As with polarity, the electrostatic potential of a simple salt depends primarily on the spatial arrangement of ions in a particular crystal structure or in solution, making a comparative trend between cofomers and a target salt difficult to discern. It is possible that more complex approaches^[35–37] based on machine learning and multivariate analysis may achieve additional discriminating power from these descriptors; however, this would require a considerably larger body of data which is not yet available for ionic cocrystals. In addition, the simple approach employed here has the benefit of giving a clear picture of the individual descriptors.

Only one trend is apparent in the screening group: AN shows a strong preference for cofomers with high packing coefficient (C_k) (Figure 4). Packing coefficient is the ratio of the volume occupied by molecules in the unit cell to the total volume of the cell and was determined for each cofomer using Equation (1):

$$C_k = (ZV_m)/V_c \quad (1)$$

where Z is the number of formula units in the cell, V_m is the volume of the molecule, and V_c is the volume of the cell. All 6 cocrystals have cofomers with packing coefficients over 83.5%, and only one cofomer above this value did not yield a cocrystal. Moreover, each cocrystal has a packing coefficient lower than those of either of the constituents. This result appears nonintuitive; the thermodynamic impetus towards more efficient packing (i.e., filling voids in crystals with low packing coefficient) is one of the central driving forces for crystallization.^[38] Even so, in the only large-scale study to assess the packing coefficients of cocrystals, Day and co-workers report that the majority of cocrystals (70%) have lower packing efficiency than their cofomers, indicating that some other

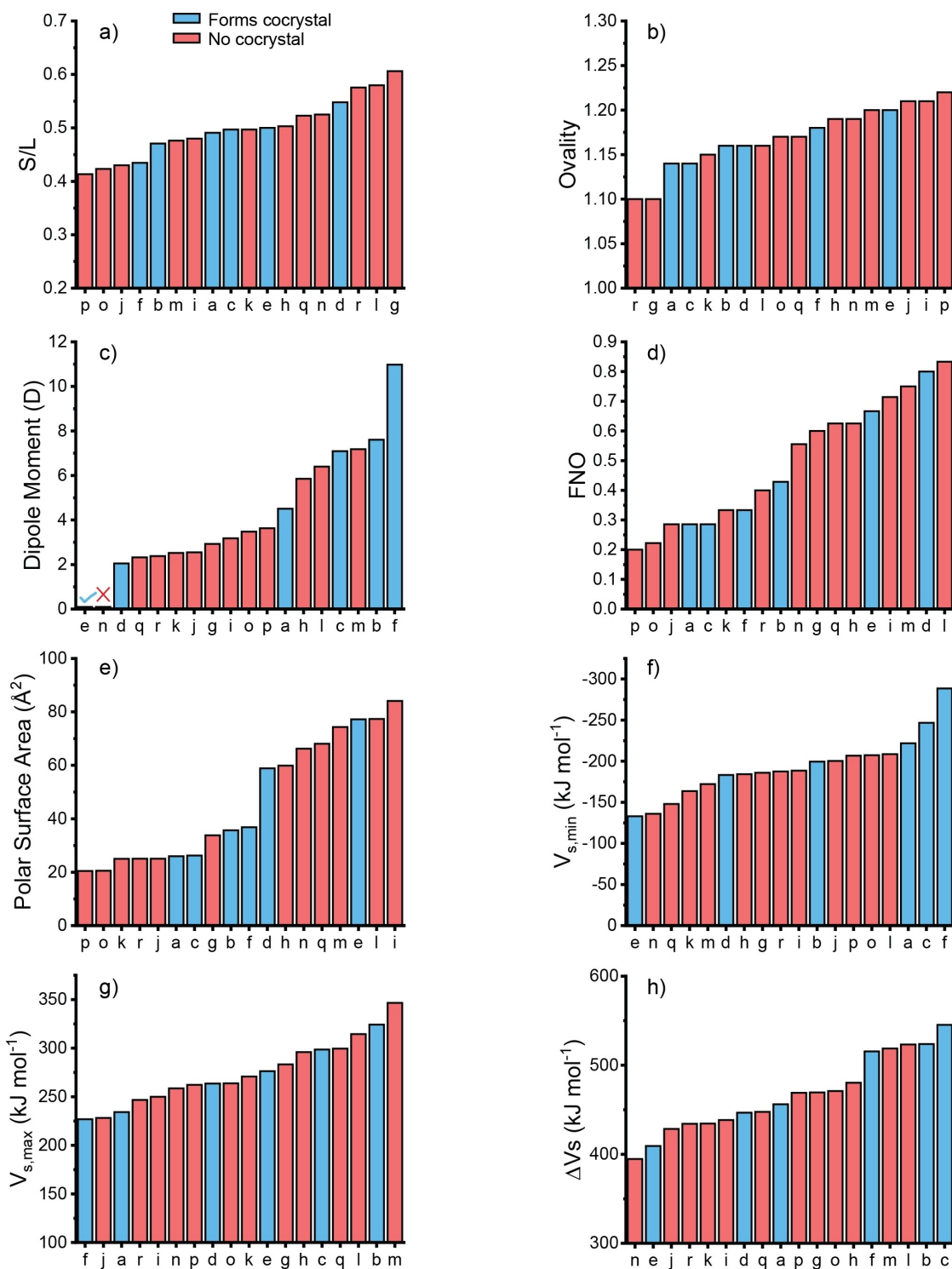


Figure 3. Bar graphs of cocystal formation versus various molecular properties of the coformers; a) short side length over long side length; b) ovality; c) dipole moment (D); d) FNO; e) polar surface area (\AA^2); f) electrostatic potential minimum (kJ mol^{-1}); g) electrostatic potential maximum (kJ mol^{-1}); h) electrostatic potential difference (kJ mol^{-1}).

thermodynamic driving force(s) may be responsible for cocrystallization.^[39] The exact reason for this trend is unknown, but it has been hypothesized that cocrystals may sacrifice some degree of packing efficiency to improve the geometry of new,

more favorable directional interactions introduced into the lattice structure. Notably, the Day study excluded ionic cocrystals from consideration. The decreased packing coefficients of our ionic cocrystals are in agreement with their

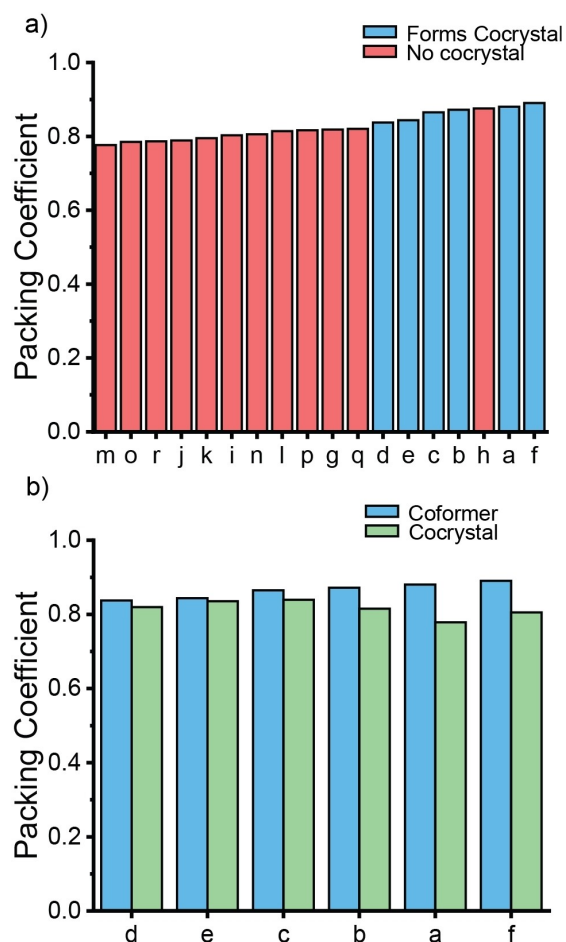


Figure 4. Bar graphs of a) coformer packing coefficient versus cocrystal formation and b) coformer packing coefficient versus cocrystal packing coefficient. AN shows a strong preference for coformers with high packing coefficient (> 83.5%). Each cocrystal also has a packing coefficient lower than that of the coformer.

findings for neutral cocrystals; however, as their dataset consists of only successful cocrystal formers, they cannot comment on the effects of packing coefficient on the likelihood of cocrystal formation. Ionic cocrystals in which the neutral coformer is a conjugate acid or base of a participating ion have previously been shown to be no more likely to form when the cocrystallizing salt has a low packing coefficient,^[34,40] further supporting the conclusion that improving packing efficiency is not an important driving force for cocrystallization. However, to our knowledge no trends (or lack thereof) have previously been reported relating the packing coefficient of the neutral coformer to the likelihood of ionic cocrystal formation. Most studies on the factors that influence cocrystallization have focused on molecular properties such as shape and polarity or chemical functionality. Within our dataset, packing coefficient of the neutral coformers appears highly relevant to ionic cocrystal success, a boon for cocrystal design in the absence of easily understood molecular properties. Indeed, packing coefficient may serve as an abstraction of some important molecular properties which are otherwise ambiguous for salts, as shape

and polarity are closely related to the allowed orientations of a molecule in its crystal structure which in turn determines their ability to pack efficiently.

After extracting the packing coefficient trend, a small second screening group of three coformers was selected based on their high packing coefficient (> 84%) and the presence of N–H functionality (Figure 5). The goal of this small-scale experiment was to demonstrate the combined effectiveness of the single-ion database approach and packing coefficient evaluation in targeting successful coformers directly, bypassing the need for large-scale screening. Applying the same experimental conditions used previously yielded AN cocrystals of 2-imidazolidone and 5-nitro-2(1H)-pyridone in 1:2 (AN:2-imidazolidone) and 1:3 (AN:5-nitro-2(1H)-pyridone) ratios, respectively. 6-Hydroxy-4(1H)-pyrimidinone exhibited very poor solubility in the solvents used in this study and yielded no cocrystal. The success of this rationally curated screening group appears to validate the observed trend in packing coefficient for ionic cocrystal formation, an important step toward enabling efficient identification of successful coformers in an emerging area of cocrystal design.

Including the second screening group, a total of eight AN cocrystals were generated. All but the picolinic acid and 2-pyridone cocrystals feature the target interaction of hydrogen bonding between nitrate and an N–H functionality on the coformer (Figure 6). Because picolinic acid is in its zwitterionic tautomer in the cocrystal, charge assisted hydrogen bonding between the carboxylate and pyridinium groups of adjacent molecules is favored over any potential nitrate interactions. The picolinic acid forms hydrogen bonded chains, staggered with AN chains to form AB stacking sheets. In the cocrystal with 2-pyridone, 2-pyridone dimerizes due to the presence of the powerful amide homosynthon, which outcompetes nitrate...coformer interactions. As a consequence, this cocrystal packs in a lamellar architecture^[21,32] with clearly defined alternating bands of 2-pyridone and AN pairs. In every other cocrystal the nitrate ion hydrogen bonds with an N–H functionality on the coformer (Figure 7). While the nitrate...H–N synthon is robust and predictably present in systems without interference from stronger synthons, it is unable to predict stoichiometry in

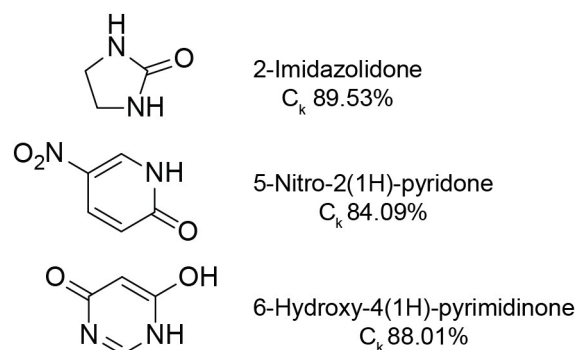


Figure 5. Three coformers targeted based on high packing coefficient and N–H functionality. 2-Imidazolidone and 5-nitro-2(1H)-pyridone successfully cocrystallized with AN.

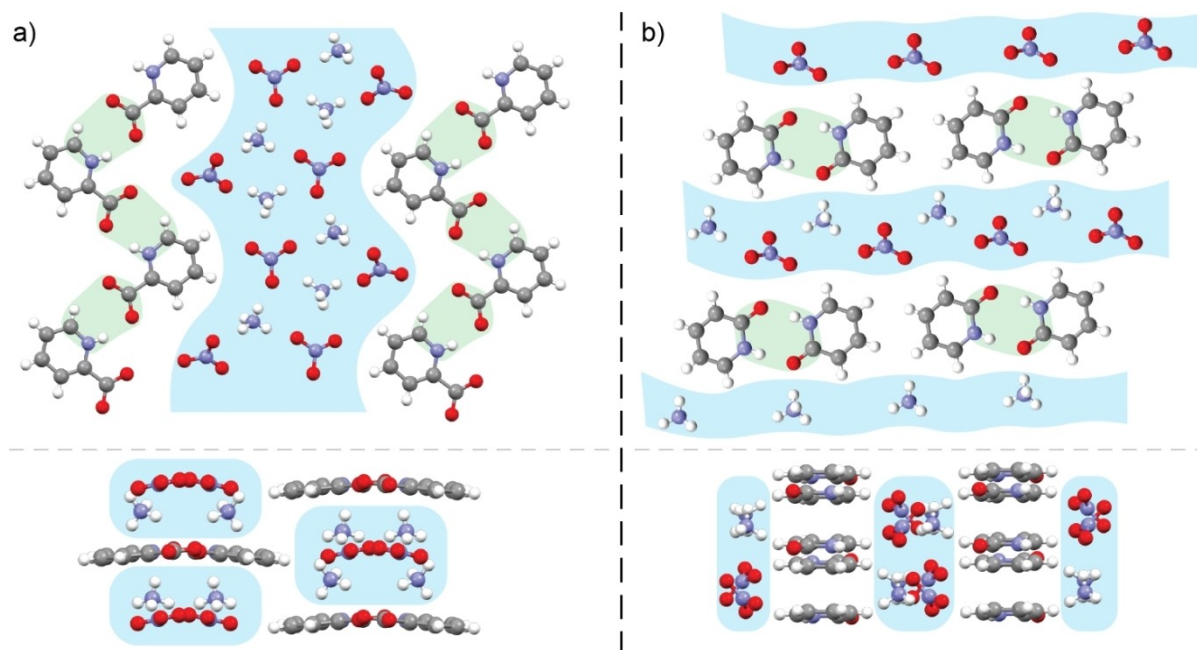


Figure 6. The targeted nitrate \cdots H–N coformer interaction does not appear in 2 out of 8 cocrystals, illustrated here with two perpendicular views. a) Picolinic acid forms infinite chains from charge-assisted H bonding between carboxylate and pyridinium groups, packing in AB sheets; b) 2-pyridone dimerizes via the powerful amide homosynthon and packs in a lamellar architecture.

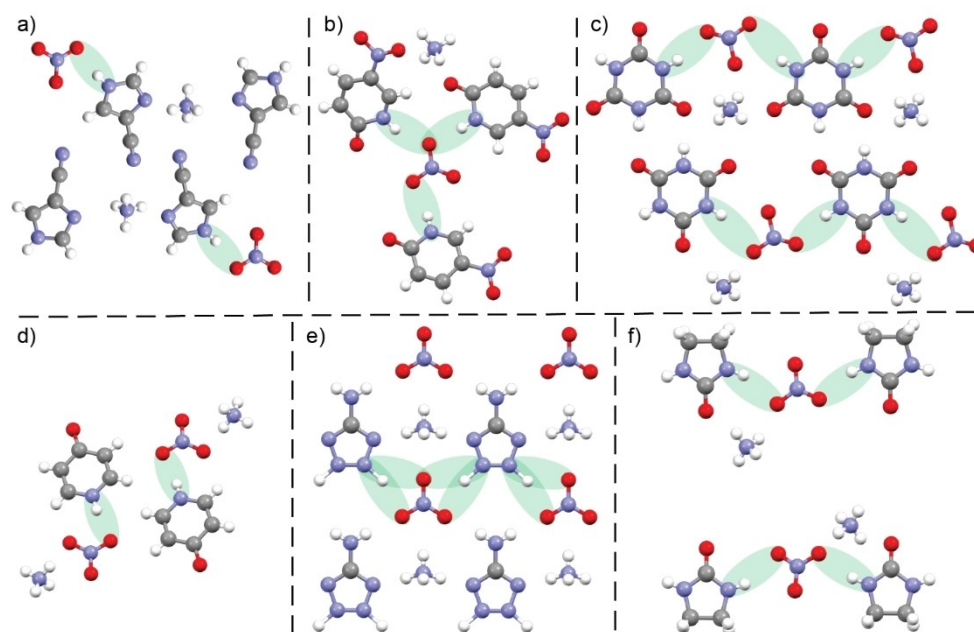


Figure 7. The targeted nitrate \cdots H–N coformer interaction is present in 6 out of 8 AN cocrystals; a) AN:4-cyanoimidazole; b) AN:5-nitro-2(1H)-pyridone; c) AN:cyanuric acid; d) AN:4-pyridone; e) AN:5-aminotriazole, in which the azolic N–H is disordered across the 2 and 3 ring positions; f) AN:2-imidazolidone.

cocrystals. Coformer molecules with multiple equivalent N–H functionalities such as cyanuric acid and 2-imidazolidone might be expected to support multiple equivalents of AN when cocrystallizing due to the potential for multiple nitrate interactions, but this was not found to be the case for the cocrystals discovered so far. Instead these coformers divide

their N–H sites between nitrate interactions and hydrogen bonding with adjacent coformer molecules. Cocrystals with two stoichiometric equivalents of coformer tended to feature coformer molecules with greater dipole moments than those that formed 1:1 cocrystals. The packing motifs enabled by these highly polar molecules are partially preserved in their cocrystals

(Figure 8). The crystal structure of 4-pyridone features chains in which the amine of one 4-pyridone hydrogen bonds with the ketone of the next. This synthon is preserved in the cocrystal in the form of a dimer, capped at both ends by AN interactions; nitrate hydrogen bonds with the exposed amine end of the pair while ammonium interacts with the exposed ketone. The crystal structure of 2-imidazolidone consists of interlocking chains of urea homosynths along the *a*- and *b*-axes. These chains persist in the cocrystal structure, but every other 2-imidazolidone has been replaced by a nitrate and two ammonium ions which spatially approximate a urea functionality. In the case of 4-cyanoimidazole, the herringbone packing and π - π stacking present in its lattice is carried over to the cocrystal, although the cyano...H-N hydrogen bond is replaced by a nitrate...H-N hydrogen bond.

Previously cocrystallization with crown ethers has been shown to stabilize AN.^[29] Differential scanning calorimetry (DSC) traces of the present cocrystals show that AN has been stabilized and the problematic phase transition eliminated in each case. In aggregate, these findings are extremely promising for creating energetic formulations based on AN; however, to maintain energetic content of the formulation, cofomers will need to be chosen with careful consideration for the oxygen balance of the resultant cocrystals.^[41]

Conclusion

The single-ion approach to cocrystal design is demonstrated as an effective tool for enabling a database approach for salts with limited representation in the CSD. In the case of ammonium nitrate, the data in consideration are increased by more than twentyfold when considering only the nitrate ion, and a nitrate...H-N interaction previously unrepresented in AN cocrystals was identified and targeted to produce eight novel AN cocrystals.

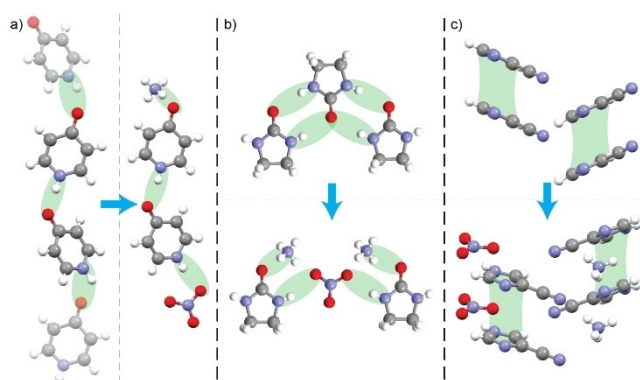


Figure 8. Successful cofomers with higher dipole moments tended to cocrystallize with two equivalents of cofomer in the cocrystal, preserving packing features present in the cofomer lattices. a) The ketone-amine homosynthon of 4-pyridone is preserved by dimers in the cocrystal; b) AN substitutes for alternate ureas in a chain of 2-imidazolidones; c) the π - π stacking and herringbone packing arrangement of 4-cyanoimidazole are preserved in the cocrystal.

The broad study of ionic cocrystals has thus far been neglected, and the establishment of guiding principles for ionic cocrystal design is a key step towards enabling applications. Previously identified trends in neutral cocrystallization were applied to the screening group but failed to explain the preference of AN for certain cofomers; many of the molecular properties typically used to predict cocrystal formation are ambiguous for salts, making comparisons between target salt and cofomer impractical. Among the successful cofomers in the group, packing coefficient greater than 83.5% is consistently observed. This trend was utilized to successfully predict the formation of two more ionic cocrystals of AN, demonstrating the combined effectiveness of the single-ion database approach and packing coefficient evaluation. Since AN also has a high packing coefficient, it is unclear at this point whether this trend is related to the absolute value of packing coefficient or, if like existing trends in shape and polarity, it depends on proximity to the target salt. Further study will illuminate whether salts with lower packing coefficients prefer to cocrystallize with cofomers with similarly low values.

Experimental Section

See the Supporting Information for synthesis and characterization of each cocrystal, computational data tables and methods, and CSD search parameters.

Deposition Number(s) 2232408, 2232409, 2232410, 2232411, 2232412, 2232413, 2232414, and 2232415 contain(s) the supplementary crystallographic data for this paper. These data are provided free of charge by the joint Cambridge Crystallographic Data Centre and Fachinformationszentrum Karlsruhe Access Structures service.

Acknowledgements

This work was supported by the ONR (Grant no. N00014-22-1-2101) and by a NASA Space Technology Graduate Research Opportunity (Grant no. 80NSSC22K1182). The authors thank Dr. Leila Foroughi and Dr. Michael Bellas for providing crystallographic expertise.

Conflict of Interest

The authors declare no conflict of interest.

Data Availability Statement

The data that support the findings of this study are openly available in the Cambridge Structural Database at <https://www.ccdc.cam.ac.uk/structures/>, reference numbers 2232408-2232415.

Keywords: crystal engineering · energetic materials · noncovalent interactions · packing coefficient · supramolecular chemistry

- [1] G. R. Desiraju, *Angew. Chem. Int. Ed. Engl.* **1995**, *34*, 2311–2327.
- [2] P. A. Wood, N. Feeder, M. Furlow, P. T. A. Galek, C. R. Groom, E. Pidcock, *CrystEngComm* **2014**, *16*, 5839–5848.
- [3] Ö. Almarsson, M. J. Zaworotko, *Chem. Commun.* **2004**, 1889–1896.
- [4] A. F. Shunnar, B. Dhokale, D. P. Karothu, D. H. Bowskill, I. J. Sugden, H. H. Hernandez, P. Naumov, S. Mohamed, *Chem. Eur. J.* **2020**, *26*, 4752–4765.
- [5] J. Hoja, H.-Y. Ko, M. A. Neumann, R. Car, R. A. DiStasio, A. Tkatchenko, *Sci. Adv.* **2019**, *5*, eaau3338.
- [6] M. E. Mswahili, M.-J. Lee, G. L. Martin, J. Kim, P. Kim, G. J. Choi, Y.-S. Jeong, *Appl. Sci.* **2021**, *11*, 1323.
- [7] M. Przybyłek, P. Cysewski, *Cryst. Growth Des.* **2018**, *18*, 3524–3534.
- [8] P. T. A. Galek, F. H. Allen, L. Fábrián, N. Feeder, *CrystEngComm* **2009**, *11*, 2634–2639.
- [9] J. J. Devogelaer, H. Meekes, E. Vlieg, R. de Gelder, *Acta Crystallogr. Sect. B* **2019**, *75*, 371–383.
- [10] N. Sarkar, J. Mitra, M. Vittengl, L. Berndt, C. B. Aakeröy, *CrystEngComm* **2020**, *22*, 6776–6779.
- [11] C. R. Groom, I. J. Bruno, M. P. Lightfoot, S. C. Ward, *Acta Crystallogr. Sect. B* **2016**, *72*, 171–179.
- [12] P. T. A. Galek, L. Fábrián, W. D. S. Motherwell, F. H. Allen, N. Feeder, *Acta Crystallogr. Sect. B* **2007**, *63*, 768–782.
- [13] J. McKenzie, C. A. Hunter, *Phys. Chem. Chem. Phys.* **2018**, *20*, 25324–25334.
- [14] L. Fábrián, *Cryst. Growth Des.* **2009**, *9*, 1436–1443.
- [15] D. Musumeci, C. A. Hunter, R. Prohens, S. Scuderi, J. F. McCabe, *Chem. Sci.* **2011**, *2*, 883–890.
- [16] T. Grecu, C. A. Hunter, E. J. Gardiner, J. F. McCabe, *Cryst. Growth Des.* **2014**, *14*, 165–171.
- [17] D. A. Haynes, J. M. Rawson, *Eur. J. Inorg. Chem.* **2018**, *2018*, 3554–3564.
- [18] M. Karimi-Jafari, L. Padrela, G. M. Walker, D. M. Croker, *Cryst. Growth Des.* **2018**, *18*, 6370–6387.
- [19] N. Schultheiss, A. Newman, *Cryst. Growth Des.* **2009**, *9*, 2950–2967.
- [20] E. Grothe, H. Meekes, E. Vlieg, J. H. ter Horst, R. de Gelder, *Cryst. Growth Des.* **2016**, *16*, 3237–3243.
- [21] M. K. Bellas, L. V. MacKenzie, A. J. Matzger, *Cryst. Growth Des.* **2021**, *21*, 3540–3546.
- [22] D. Braga, F. Grepioni, G. I. Lampronti, L. Maini, A. Turrina, *Cryst. Growth Des.* **2011**, *11*, 5621–5627.
- [23] D. Braga, F. Grepioni, O. Shemchuk, *CrystEngComm* **2018**, *20*, 2212–2220.
- [24] X. Zhang, S. Chen, Y. Wu, S. Jin, X. Wang, Y. Wang, F. Shang, K. Chen, J. Du, Q. Shu, *Chem. Commun.* **2018**, *54*, 13268–13270.
- [25] K. Inoue, K. Okada, M. Kumasaki, K. Usuki, *J. Energ. Mater.* **2022**, *0*, 1–13.
- [26] M. Kohga, T. Naya, K. Okamoto, *Int. J. Aerosp. Eng.* **2012**, *2012*, e378483.
- [27] D. Trache, T. M. Klapötke, L. Maiz, M. Abd-Elghany, L. T. DeLuca, *Green Chem.* **2017**, *19*, 4711–4736.
- [28] C. Oommen, S. R. Jain, *J. Hazard. Mater.* **1999**, *67*, 253–281.
- [29] T. Lee, J. W. Chen, H. L. Lee, T. Y. Lin, Y. C. Tsai, S.-L. Cheng, S.-W. Lee, J.-C. Hu, L.-T. Chen, *Chem. Eng. J.* **2013**, *225*, 809–817.
- [30] V. H. Rodrigues, M. Ramos Silva, A. Matos Beja, J. A. Paixão, M. M. R. R. Costa, *Acta Crystallogr. Sect. E* **2005**, *61*, o1631–o1633.
- [31] K. M. Doxsee, P. E. Francis, T. J. R. Weakley, *Tetrahedron* **2000**, *56*, 6683–6691.
- [32] M. K. Bellas, A. J. Matzger, *Chem. Sci.* **2022**, *13*, 12100–12106.
- [33] G. Chen, M. Jiang, *Chem. Soc. Rev.* **2011**, *40*, 2254–2266.
- [34] T. Alkhalid, Z. M. Saeed, A. F. Shunnar, E. Abujami, R. M. Nyadzayo, B. Dhokale, S. Mohamed, *Cryst. Growth Des.* **2022**, *22*, 485–496.
- [35] J.-J. Devogelaer, H. Meekes, P. Tinnemans, E. Vlieg, R. de Gelder, *Angew. Chem. Int. Ed.* **2020**, *59*, 21711–21718; *Angew. Chem.* **2020**, *132*, 21895–21902.
- [36] M. Przybyłek, T. Jeliński, J. Stabuszewska, D. Ziolkowska, K. Mroczńska, P. Cysewski, *Cryst. Growth Des.* **2019**, *19*, 3876–3887.
- [37] D. Wang, Z. Yang, B. Zhu, X. Mei, X. Luo, *Cryst. Growth Des.* **2020**, *20*, 6610–6621.
- [38] A. I. Kitaigorodskii, *Acta Crystallogr.* **1965**, *18*, 585–590.
- [39] C. R. Taylor, G. M. Day, *Cryst. Growth Des.* **2018**, *18*, 892–904.
- [40] S. Mohamed, A. A. Alwan, T. Friščić, A. J. Morris, M. Arhangelskis, *Faraday Discuss.* **2018**, *211*, 401–424.
- [41] J. C. Bennion, A. J. Matzger, *Acc. Chem. Res.* **2021**, *54*, 1699–1710.

Manuscript received: January 9, 2023
Accepted manuscript online: February 22, 2023
Version of record online: March 30, 2023